論 文

Numerical Simulation for the Prediction of Microstructural Evolution in Steels during Various Heat Treatments

Si-Young Kwahk† and Jeong-Kil Choi*

Abstract

본 연구에서는 여러 다른 냉각속도로 냉각되는 강의 조직과 경도를 예측하는 수치 해석을 수행하였다. 해석 프로그램은 확산과 비확산 변태에 대한 변태 이행 방정식과 유한차분법을 이용하여 제품에 대해서 온도분포 및 조직변태에 대한 예측을 수행하고 또한 경도를 예측하도록 하였다. 해석 결과와의 비교를 위해 여러 다른 냉각속도로 냉각되는 AISI 410시편들에 대한 일련의 실험을 행하여 각각의 조직과 경도를 구하였으며 특히 온도해석에 사용하는 열전달계수는 실험을 통하여 구한 값을 사용하였다. 실험에 의해 구해진 결과는 해석 프로그램을 이용한 값과 잘 일치 하였다.

(Received April 30, 2001)

Keywords : Microstructure evolution, FDM, AISI 410, Hardness

1. Introduction

Although heat treatment is a process of great technological importance in order to obtain desired mechanical properties such as hardness, these processes were required a tedious and expensive experimentation to specify the process parameters. Consequently, the availability of reliable and efficient numerical simulation program would enable easy specification of process parameters to achieve desired microstructure and mechanical properties.

Since typical heat treatment processes such as annealing, tempering and quenching are performed under an isothermal or anisothermal cooling, the prediction of microstructure in metal is made difficult by the complex nature of the coupled heat transfer and microstructure transformation kinetics. In spite of this complexity in analysis, a number of studies have dealt with the prediction of microstructure evolutions and mechanical properties in steels during these thermo-mechanical processes. A brief review is given in references [1,2].

In present work, the developed numerical simulation program could predict the microstructure and hardness in steels under cooling condition. The computer program is based on the finite difference method for temperature analysis and microstructure evolutions.

To begin with the paper introduces the microstructure evolution equations, then provides finite difference procedure for heat transfer and microstructure evolutions. Next experimental section describes the technique adopted in the present study for evaluation the convection heat transfer coefficient. The convection heat transfer coefficient was calculated by the trial-and-error method using the experimental temperature history and simulation result.

Finally the simulation program was verified by previously published results[2] of AISI 1080 carbon steel and compared with experimental results in AISI 410 stainless steel specimens having various cooling rates.

2. Microstructure Evolution Model

Department of Mechanical Engineering , INHA University, Inchon Korea
*Korea Institute of Industrial Technology, Inchon Korea
†E-mail : vlvwlw@netian.com

2.1 Austenite Pearlite transformation

Austenite Pearlite transformation is diffusion transformation. The kinetics of the diffusion transformation are described by Avrami type equation[3]. Thus the volume fraction of pearlite F_p can be written as

$$F_p^{t+\Delta t} = 1 - exp(-B_p(T)\theta_j^{N_p(T)}) \quad (1)$$

where $B_p(T)$ and $N_p(T)$ are material parameters that were calculated from the isothermal Time-Temperature-Transformation diagram(TTT) for the material. The values of $B_p(T)$ and $N_p(T)$ are obtained by the expression [2,4]

$$N_p(T) = \frac{ln\left[\frac{ln(1-F_s)}{ln(1-F_e)}\right]}{ln\left[\frac{\theta_s}{\theta_e}\right]} \quad (2)$$

$$B_p(T) = \frac{ln(1-F_s)}{\theta_s^{N_p(T)}} \quad (3)$$

Here θ_s and θ_e are the starting and finishing times for a transformation, and F_s and F_e the starting and finishing volume fractions.

The transformation time θ_j, the time elapsed from the beginning of the diffusion transformation, is obtained by the form based on the volume fraction of the phase F_p present at the previous time step (j-1) :

$$\theta_j = \Delta t_j + \left[\frac{ln(1/(1-F_p(j-1)))}{B_p(T)}\right]^{\frac{1}{N_p(T)}} \quad (4)$$

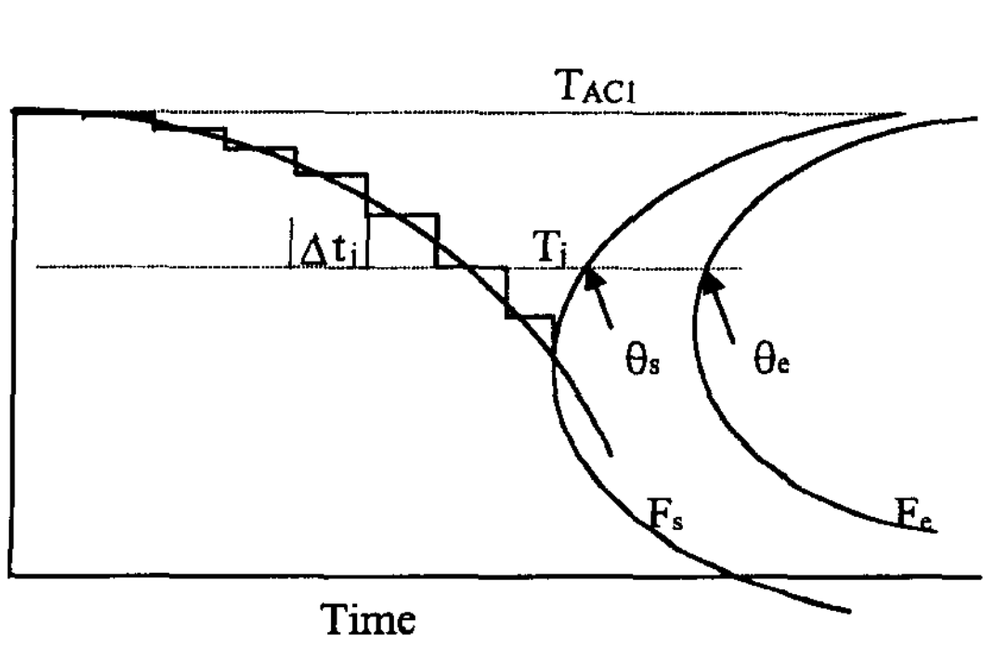

Fig. 1. The transformation parameters on TTT diagram.

where Δt_j is current time step, j is current iteration time step. The symbols θ_s, θ_e and Δt_j on a TTT diagram are described in Fig. 1.

Scheil's principle is used to estimate the incubation period for diffusion transformation. For each time step j, the value of $\Delta t_j/\theta s(T_j)$ is calculated and summed. Then the start of transformation occurs when the following condition is fulfilled.

$$\Sigma\frac{\Delta t_j}{\theta_s(T_j)} = 1 \quad (5)$$

2.2 Austenite-Martensite Transformation

The martensitic transformation is not diffusion controlled and its evolution equation is different from that for the pearlitic transformation equation. The fraction of martensite F_m formed at a given temperature is estimated by Koistinen and Marburger law[2]

$$F_m = [1 - exp[-\bar{\alpha}(T_{ms} - T)]]\left[1 - \sum_i F_i\right] \quad (6)$$

where $\bar{\alpha} = 1.10\times10^{-2}\,^{o}K^{-1}$. The value of T_{ms} is martensite start temperature. And the summation is carried out over all the non-martensitic phase.

2.3 Mechanical Properties

As well known, a typical microstructure for steels is composed of several phases. The material properties, P, at a point were assumed to be a linear combination of the corresponding properties, P_i ,of each phase weighted proportional to the volume fraction F_i of the phase at present point. Thus any material property, P, of material can be written as

$$P(F_i, T) = \sum_i P_i(T)F_i \quad (7)$$

where the summation is carried out over the total number of phase.

3. Computational Procedure

3.1 Temperature Analysis

The transient heat conduction equation for a solid with an internal heat source is

$$\nabla(k\nabla T) + \dot{q} = \rho C_p \frac{\partial T}{\partial t} \tag{8}$$

where k, ρ, and C_p are the thermal conductivity, density and specific heat of the solid, and $\dot{q}$ is the rate of heat generation within the material.

The convective boundary conditions for the problem at the free surface of the workpiece are given by

$$-k\nabla T = h(T)(T_\infty - T_s) \tag{9}$$

where h(T) is the convective heat transfer coefficient.

$\dot{q}$ is the internal heat source due to the enthalpy changes occurring during the phase transformations. This can be expressed as

$$\dot{q} = \sum_i \Delta H_i \frac{\Delta F_i(T)}{\Delta t} \tag{10}$$

where ΔH_i is the latent heat released when a phase, i, is formed.

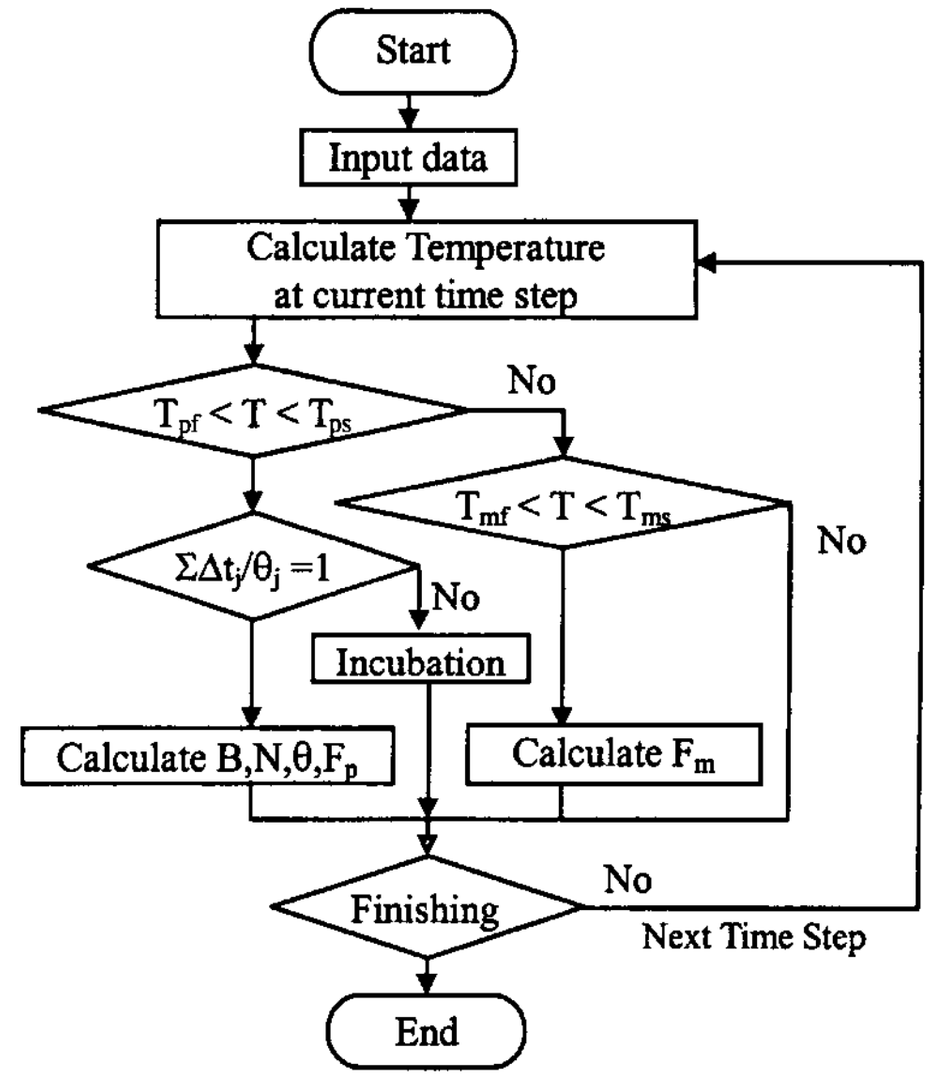

Fig. 2. Flow chart of the simulation procedure for microstructure prediction.

3.2 Finite Difference Formulation

The amount of heat-change(Q_a) in an element, i, during the time step Δt is

$$Q_a = \frac{\rho c}{\Delta t} V_i (T_i^{t+\Delta t} - T_i^t) \tag{11}$$

The heat quantity (Q_b) transferred through the boundary between an considered element, i, and a neighbor element, j, is given by

$$Q_b = \sum_i \sum_{j(\neq i)} B_{ij} \cdot A_{ij} (T_j^t - T_i^t) \tag{12}$$

where A_{ij} and B_{ij} are respectively, the boundary face, the boundary condition between the element i and j. And B_{ij} is calculated by the geometry and materials of neighbor elements[5].

The calculation procedure including microstructure prediction is summarized in the flow chart of Fig. 2.

4. Experimental Work

AISI 410 stainless steel specimens, which are 25 mm × 35 mm × 45 mm in size, were used for this experiment. And the composition is 0.13% C, 0.35% Si, 0.4% Mo and 13.62% Cr.

In this experiment, the specimens were divided into two groups - group A and B. The group A had two different cooling curves, one had fast cooling curve which makes martensite structure in the specimen(group A-1) and the other had very slow cooling curve which makes fully pearlite in the specimen(group A-2). The Brinell hardness test was carried out for group A-1 and group A-2 then ; the hardness values of fully martensite and pearlite were obtained. The above values were used for prediction hardness in numerical simulation later.

The two specimens belong to group B underwent different cooling rates so that the specimens had different structures each other. The different cooling rates induce the specimens to be a variety of microstructures while the size of specimen is small so that the microstructure of that was assumed to be the same over whole part. Fig. 3 shows the cooling curves for these specimens.

A K-type thermo-couple was located in the center of 50 mm × 50 mm × 50 mm size specimen in order to obtain the temperature history of specimen during cooling. Using this temperature history, the convection heat transfer coefficient for this experiment was obtained.

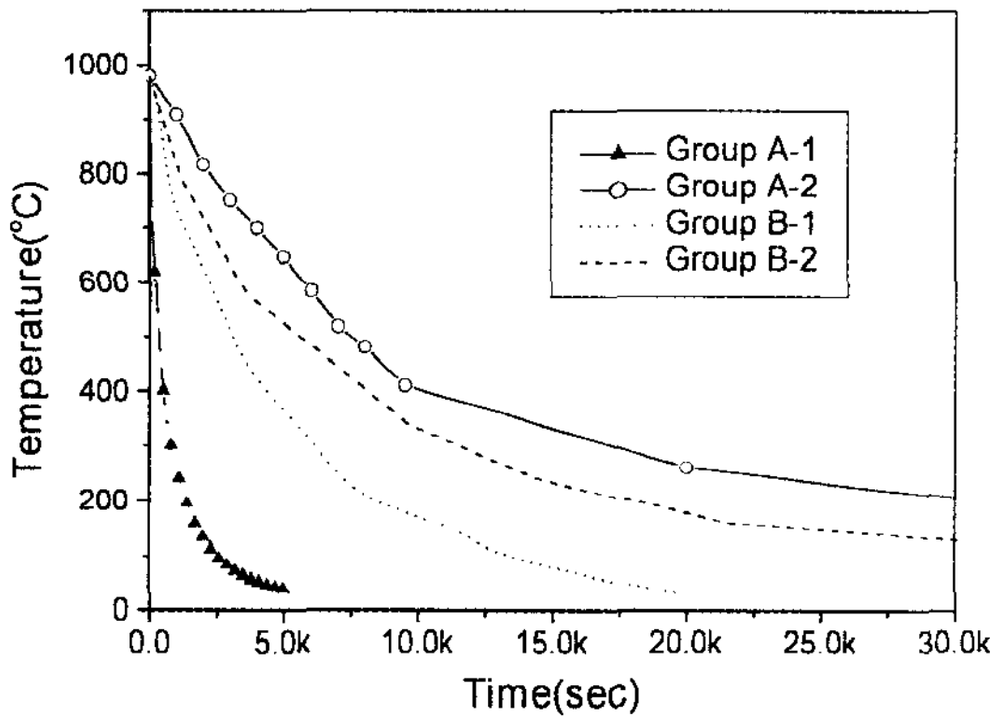

Fig. 3. The thermal histories of AISI 410 specimens in experiment.

The specimens were heated to 980°C for four hours and kept at that temperature for two hours to ensure that the matrix was completely austenitized. Then they were cooled with different cooling rate in the air.

5. Results and discussion

5.1 Simulation program verification

To verify the present finite difference formulation and simulation procedure, the simulation of quenching of AISI 1080 carbon steel cylinder was carried out. And the result of this problem was compared with that of Wang[2] who carried out the experiment and simulation for the problem.

The steel cylinder used in the simulation was 38 mm in diameter and 250 mm long. The initial temperature was assumed to be 850°C and the temperature of the surrounding quenchant was assumed to be 22.5°C. The thermophysical properties, TTT diagram of the AISI 1080 steel and heat transfer coefficient was the same as those used by the above reference.

Fig. 4 shows the fraction of pearlite and martensite along the radial direction for cylinder after the whole cylinder has reached room temperature. The lines without any symbol refer to the results of the simulation developed in this study, and the symbols refer to the results of reference. The two results agreed well with each other.

5.2 The convection heat transfer coefficient in air cooling

Based on thermocouple measurements of the cooling at the center of the specimen, the convection heat transfer coefficient for this experiment was obtained iteratively using the present simulation; the convective heat transfer coefficient is varied in a simulation of specimen model until the calculated cooling curve matches the measured curve. Fig. 5 shows the convective heat transfer coefficient obtained by the above method.

5.3 Experiment and Simulation results

Fig. 6 shows optical micrographs of the microstructs for group A; (a) is the martensite structure by fast cooling and (b) is the pearlite structure by very slow

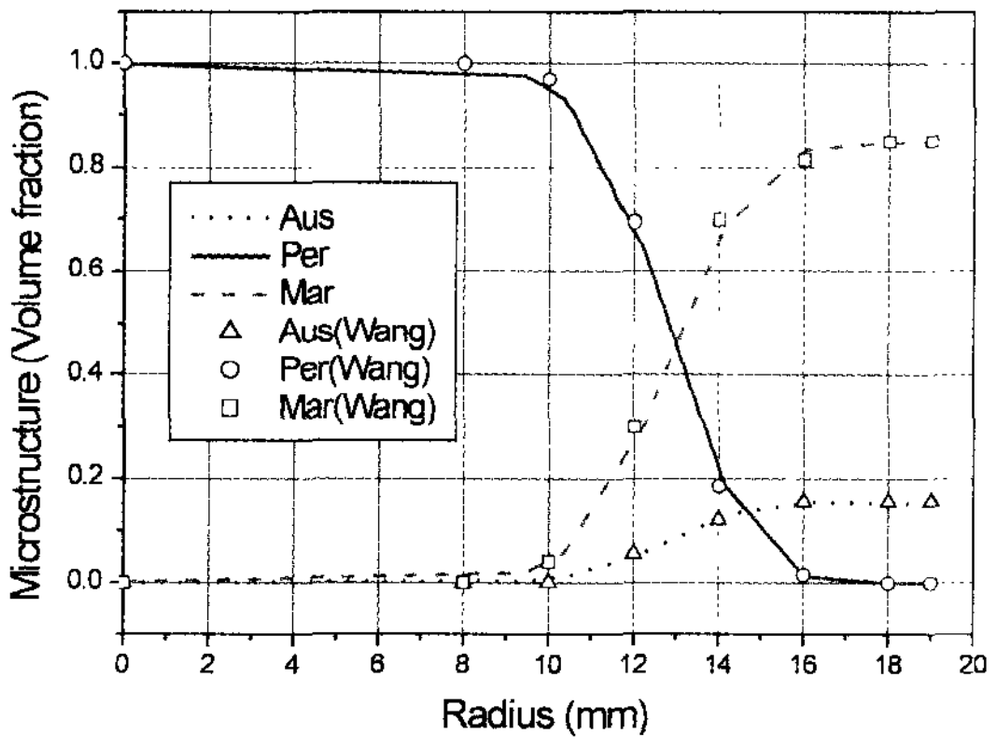

Fig. 4. The microstructure along the radial direction from the center after quenching in the water.

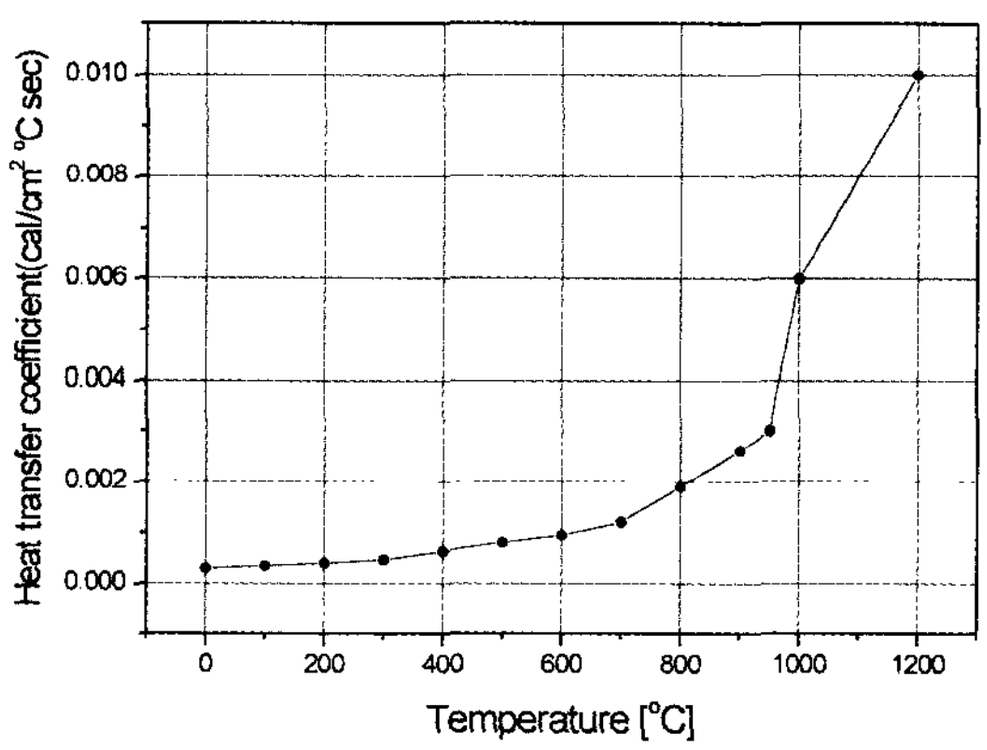

Fig. 5. The convection heat transfer coefficient for the cooling of AISI 410 in the air.

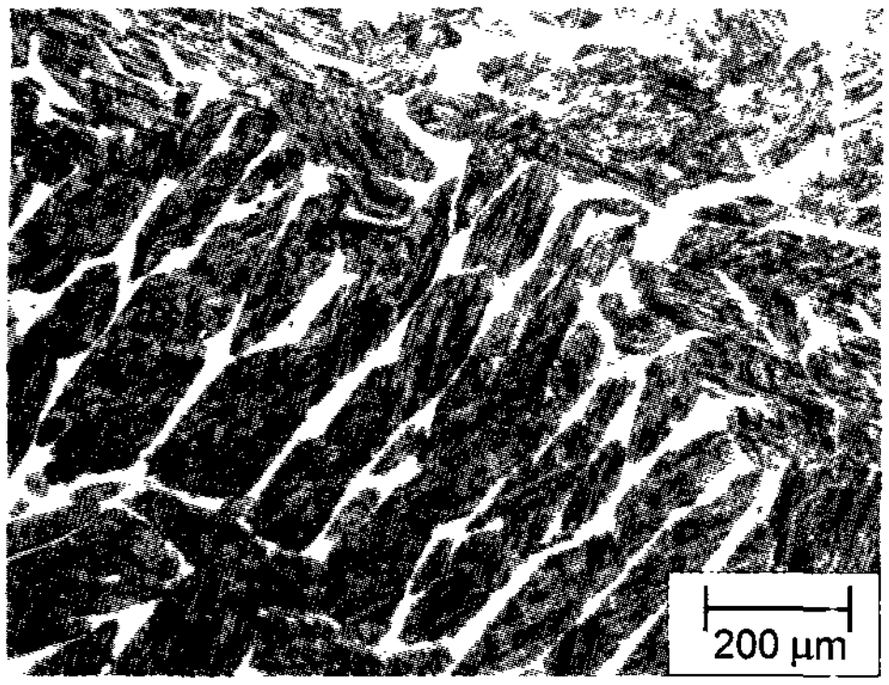

(a)

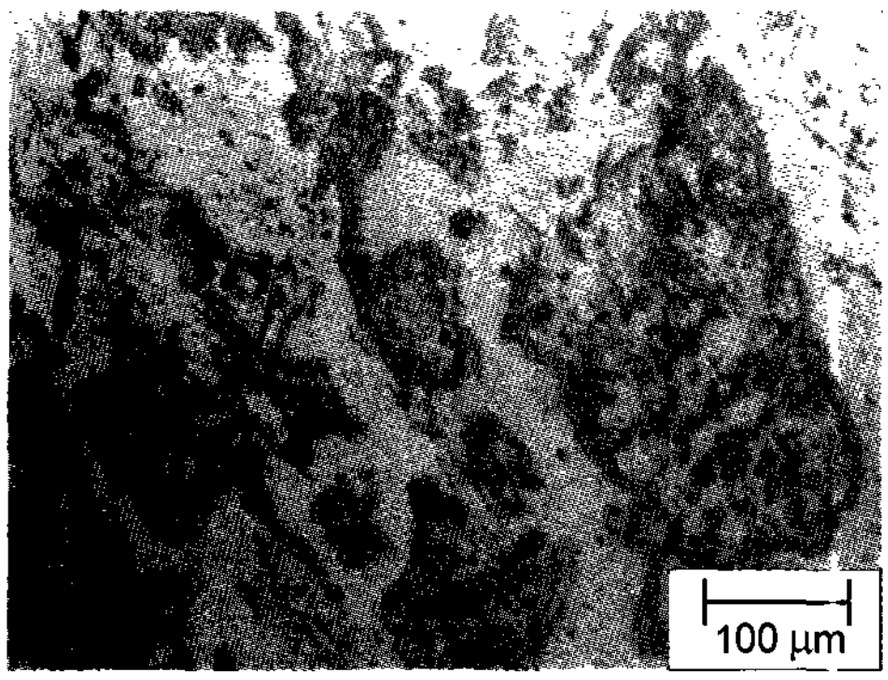

(b)

Fig. 6. Optical micrographs of AISI 410 stainless steel. Vilellas reagent; (a) Martensite (× 100) and (b) Pearlite (× 200).

cooling. The Brinell measurement for hardness used a 10 mm ball and 3000 kg load. The values of Brinell hardness are 316 HB, 156 HB respectively.

The two specimens belong to group B which undergo different cooling rate have different volume fractions of the pearlite and martensite. But it is difficult to decide the exact volume fraction of pearlite and martensite at each specimen through optical micrographs. So the hardeness of the specimens was measured. The hardeness values of group B-1 and group B-2 are 183 HB, 258 HB respectively. These values of the hardness are compared with the simulation results later.

The computer simulation was carried out using the TTT diagram of AISI 410 shown in Fig. 7, thermo-physical properties[6,7] and the convection heat transfer coefficient in Fig 4. The simulation results present in Table 1. In this table , the calculated hardness was evaluated by Eq. (7).

Table 1. The results of simulation for prediction microstructure of AISI 410

	Calculated microstructure	Calculated Hardness[HB]
Group B-1	Martensite 21.7 % Pearlite 77 %	193.6
Group B-2	Martensite 72.4 % Pearlite 23.8%	271

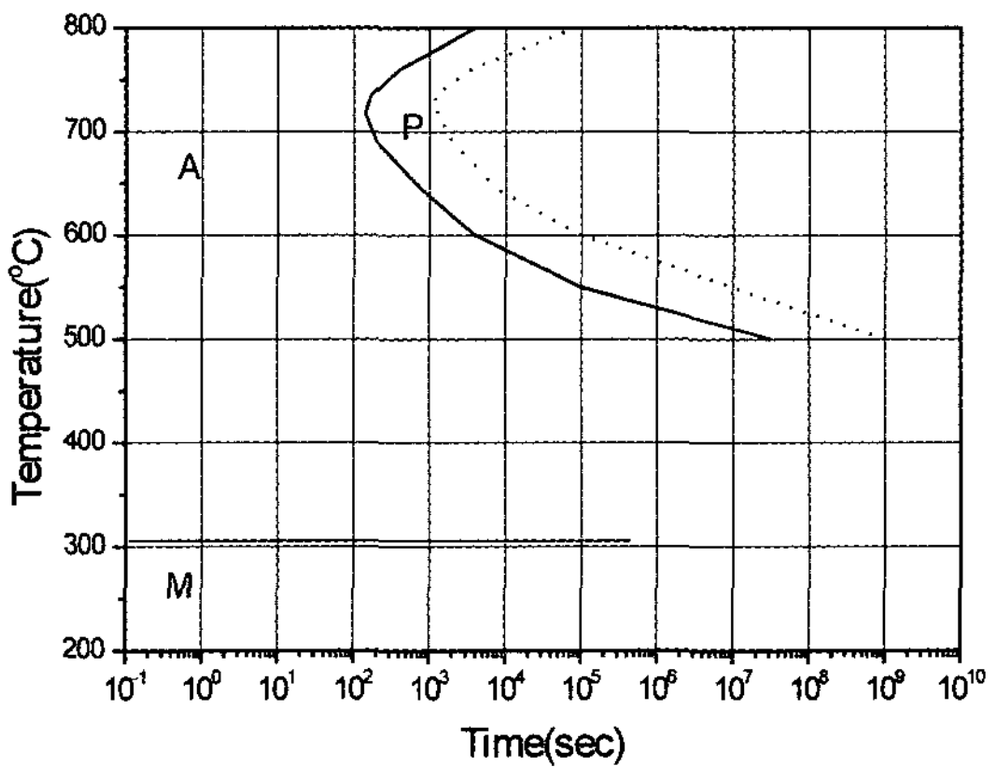

A : Austenite, P : Pearlite, M : Martensite

Fig. 7. TTT diagram for simulation of AISI 410.

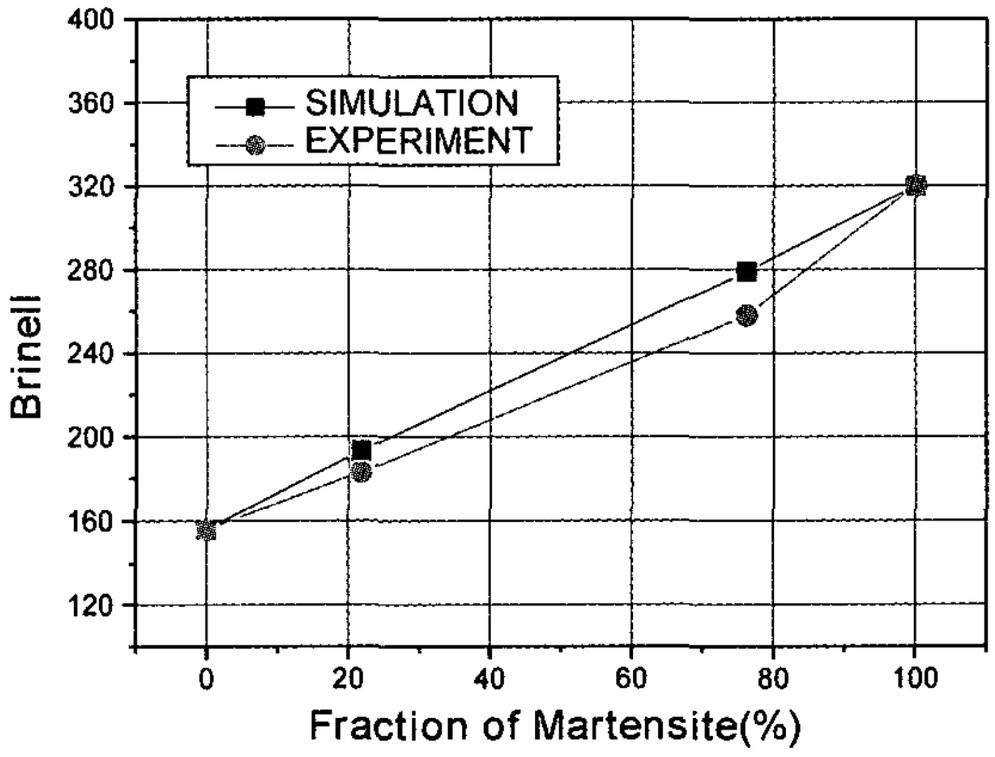

Fig. 8. The calculated and measured hardness in AISI 410 stainless steel.

Fig. 8 shows a comparison of the predicted and measured hardness in specimens with the different martensite volume percent. It must be pointed out here that the hardness of pearlite in general is dependent upon the grain size and temperature at which it is formed. However in our model at present this dependency is not

considered. The retained austenite, ferrite and the latent heat for AISI 410 are not considered in this model. These induce discrepancy between calculated and measured hardness. But the result shows that the simulation is applicable in industrial field.

6. Conclusions

The computer simulation program has been developed to predict the microstructure and hardness of steels during the cooling. The program was checked against previously published results and in the case of AISI 410 the predicted results were compared with those of experiment. These comparisons gave satisfactory result.

The developed finite difference procedure provides a powerful tool to determine the cooling process parameters and to design the microstructure and hardness variation. The productivity would go up when the program is applied in analysis of industrial parts large or complex in geometry. And it is easy to extend the program to dealing with other steels of which microstructure evolution is similar to that of plain carbon steel.

In further work, the simulation program would be extended to the prediction of residual stress during heat treatment, and studies on stresses would lead to a complete stress-transformation-thermal history coupling analysis.

References

[1] F. M. B. Fernandes, S. Denis and A. Simon, Mathematical model coupling phase transformation and temperature evolution during quenching of steels, Materials Science and Technology, Vol. 1, October (1985) 838

[2] K. F. Wang, Analysis of the Carburization and Quenching of steels, Ph D Thesis, (1996)

[3] M. Avrami, "Kinectics of Phase Change II", J.Chem. Phys., Vol. 8, (1940) 212

[4] P. K. Agarwal and J. K. Brimacombe, Mathematical Model of Heat Flow and Austenite Pearlite Transformation in Eutectoid Carbon Steel Rods for Wire, Metallurgical Transactions, Vol 12B, March (1881) 121

[5] J. K. Choi, Prediction of Casting Defects and Control of Casting Process by Computer Simulation, Ph D Thesis, 1992 (4)

[6] Stainless Steel Handbook, NIKKAN KOGYO SHIMBUN, LTD., (1984)

[7] High-Temperature Property Data: Ferrous Alloys, ASM International, (1988)